



Engineering geological appraisal of relative stability of Akure – Ondo Highway segment of F-209, Southwestern Nigeria: Post-Construction analysis

Olumuyiwa Olusola Falowo ^{*1,2}, Abayomi Solomon Daramola ²

¹Rufus Giwa Polytechnic Owo, Department of Civil Engineering Technology, Ondo State, Nigeria, solageo2018@gmail.com

²Federal University of Technology, Akure, Department of Applied Geology, Ondo State, Nigeria, mogfalowo@yahoo.co.uk

Cite this study: Falowo, O. O., & Daramola, A. S. (2023). Engineering geological appraisal of relative stability of Akure – Ondo Highway Segment of F-209, Southwestern Nigeria: Post-Construction analysis. *Engineering Applications*, 2 (2), 94-114

Keywords

DCPT
Resilient modulus
Elastic modulus
Trial pit
Resistivity

Research Article

Received:15.03.2023
Revised: 29.04.2023
Accepted:10.05.2023
Published:26.05.2023



Abstract

The study examined the relative stability of Akure – Ondo which is a segment of F-209 Highway in Ondo State, southwestern Nigeria using geoen지니어ing method. Investigation showed that the pavement is founded on sandy clay, sand and laterite. The average silica-sesquioxide ratio of the sample is 1.63 (lateritic soil type) with activity of 0.69 (inactive clay), while the clay mineralogy group is illite, and soaked California Bearing Ratio (CBR) is 12%. Thus, the thickness of the pavement should range from 325 mm (good segment) to 518 mm (for weak segment), which is far above the 192 – 316 mm existing thickness of the highway structure. In the upper 1.0 m, the subgrade structural number (SNG) coefficient for subgrade soil is higher than 0.5. The strength coefficient of the soil as subbase and base is less than 0.5. Therefore, based on these results, it can be concluded that the relative stability of the highway is due to its good engineering properties. The regression models of all parameters gave strong positive correlations for all the parameters correlated: soaked CBR and in-situ CBR, elasticity modulus and resilient modulus, in-situ CBR and resilient modulus, relative density and penetrative index, and relative density and in-situ CBR. However imminent failure is expected due to deficit in the design thickness and lack of drainage facility at the shoulders of the highway. The haulage activities along the highway have increased tremendous of recent; definitely it will affect the stability of the structure since its design-thickness will not sustain the present loadings on the highway in the long run.

1. Introduction

The rate of economic growth in a nation has been linked to have direct proportionality with rate at which the transport sector develops [1-2]. Hence the place of transport in nation's building cannot be overemphasized in assessment of the overall Gross Domestic Product (GDP). A good transport system facilitates good administration of a country, it determines cost of commodities or goods, it improves agriculture (in terms of supply of inputs, seedling, fertilizer, labour and machinery, helps in industrialization and transportation of raw materials, preservation of quality of goods and bye-products or finished goods, enhances urbanization, it also serves as medium of exploitation of natural resources [3-6]. Akure – Ondo is a segment of F-209 highway owned by the Federal Government of Nigeria. It is one the highways in Ondo State that is relatively stable over the years. Even though the effort of Federal Road Maintenance Agency (FERMA) is felt at different times along the highway. However, this will not underestimate its stability, since maintenance is one of the phases of road preservation. Due to the relative stability of the highway, it is improving the socio-economic development area through which the road cut across. In this study, the dynamic cone penetration test in complimentary non-destructive and/or semi-destructive and laboratory subsoil test [7-9] have been on increase in pavement structural characterization. This

is applicable to all pavement types, by determining the strength and stability properties of the unbound layers, which play a vital role in highway performance and serviceability [10-12].

Over the years, excavation, coring and laboratory soil analysis have been used to estimate the thickness and bearing capacity in terms of California Bearing Ratio (CBR) of pavement layers [13-14]. However, these methods are destructive and can have significant impact on pavement performance [15-16]. This leads to invention of non-destructive test or semi-destructive equipment for pavement analysis. The overall objectives of these tests are to obtain mechanical and engineering properties of structural layers in relation to their stability or competence [17-19]. Although, the non-destructive test cannot replace conventional boring or excavation, but it will compliment it [20-21]. Many scholars have shown the usefulness of non-destructive test, and excavation combined with laboratory studies in probing subgrade, subbase/base layers [3, 8-10, 22-24]. Many correlations were developed between CBR and Dynamic Cone Penetration test (DCPT) penetrative index (DCPI), CBR and resilient modulus (MR), MR and elastic modulus (ER) [25-30].

Subsequently, the objectives of this study are to identify and classify the subsoil within the road alignment; assess the subsoil geological, geochemical, and geotechnical properties in relation to relative stability of the soil domain based on destructive and non-destructive in-situ tests/survey and laboratory studies; determine important geotechnical correlations and parameters modeling for the highway; investigate any geological structure that could be inimical to stability of the highway structure presently and in the future.

2. Material and Method

2.1. Study area

The Akure – Ondo highway is located within Ondo State central senatorial district in southwestern Nigeria, connecting the central to the southern and northern parts of the State, and to Ore, Benin, Ife, and Lagos State (Figure 1). The road is about 45 km stretch of F-209 starting from Ondo garage in Akure (coordinates: 737677 mE, 802000 mN; elevation of 341 m) to Ife garage (704860 mE, 786577 mN; elevation 251 m) of the highway. The highway is generally flat, although few segments are hilly. The highway falls within the tropical rainforest climate characterized by rainy and dry seasons. The rainy season starts in March to October, while the dry season commences in November and ends in February. The average annual rainfall and temperature are 1800 mm and 27 °C [31-32] respectively. The months of June and Septembers usually experience heavy rainfall with relative humidity of about 80 %, although could be less than 50 % during the dry season [31].

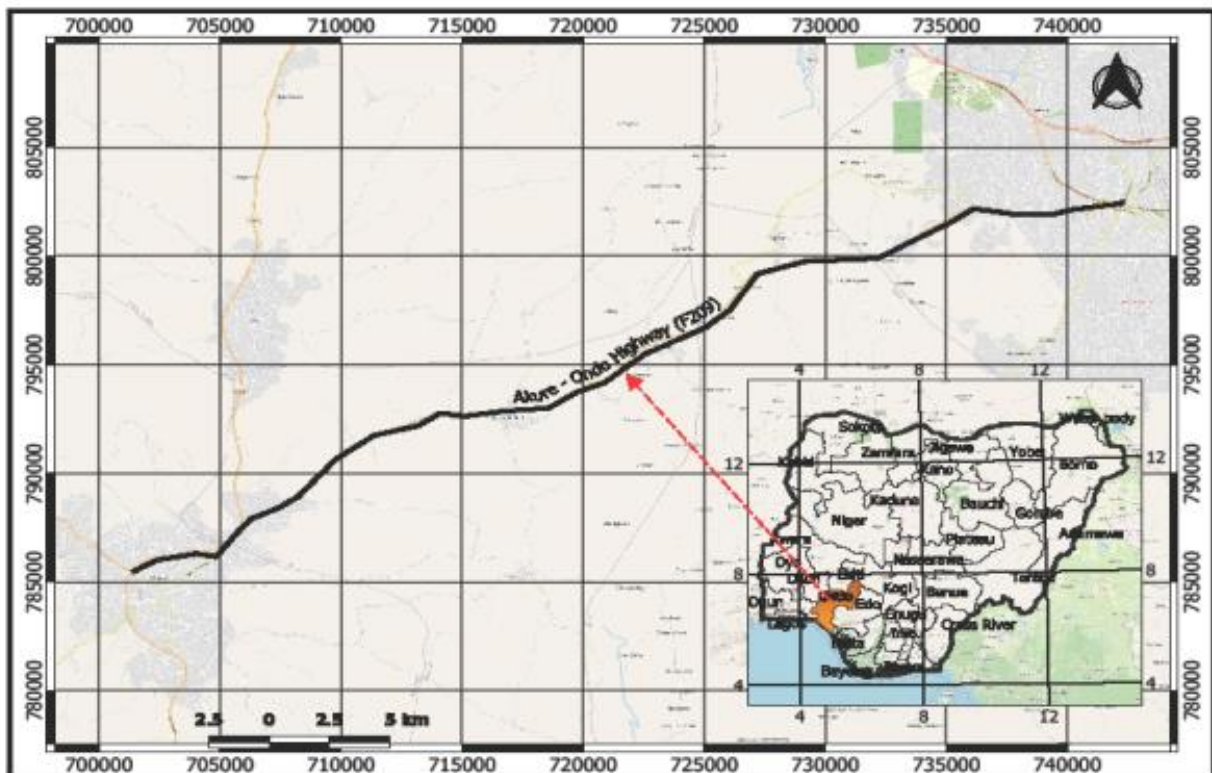


Figure 1. Map of the Studied Highway. Inset: Map of Nigeria showing the location of Akure – Ondo Highway in southwestern Nigeria

2.2. Geology and soil

Geologically, the highway is underlain by the Precambrian southwestern Basement Complex rocks, with migmatites, biotite granite, and gneiss being the major rocks observed within the highway alignment (Figures 2 and 3). They occur as range of hills of low - moderate altitude. The gneiss is banded with parallel alternation of light and colored minerals. The migmatite gneiss is strongly foliated, composing of biotite, hornblende, quartz and feldspar. The highway fall within the Ondo soil association type [33], which are weathered products of medium grained granites and gneisses, it is well drained, of medium to fine textured, orange brown to brownish red, fairly clayey soils overlying orange, brown and red mottled clay. Along the highway, no noticeable side drainage was observed, but the area is characterized by dendritic and trellised drainage systems.

The methods adopted are categorized into two phases, namely field work/survey and laboratory soil analysis. Before the commencement of the phases, there was literature review of available geological, geotechnical, hydrogeological, highway, and transportation articles or text as related to this study [34-35]. The field work involved electrical resistivity survey using vertical electrical sounding technique, in-situ dynamic cone penetrometer test, soil excavation in form of pits and trenches, water table measurement of wells in close proximity to the highway [7, 36] and identification of spring/artesian well system (if any). The data acquisition map for the study is shown in Figure 4. The geophysical investigation helps to detect zone of anomalies by measuring variation in subsurface condition [15]. They are used to determine the geological sequence and structure of subsurface rocks/soils by the measurement of certain physical properties [37]. The properties that are made most use of in geophysical exploration are density, elasticity, electrical conductivity, magnetic susceptibility and gravitational attraction [38-39]. In this study, electrical resistivity (vertical electrical sounding) was utilized at five locations along the highway. In this method an electric current is introduced into the ground by means of two current electrodes and the potential difference between two potential electrodes is measured. For this study, the resistivity - meter used was able to measure the apparent resistance directly in ohms rather than observing both current and voltage. The schlumberger array was used at half current spacing of 65 m.

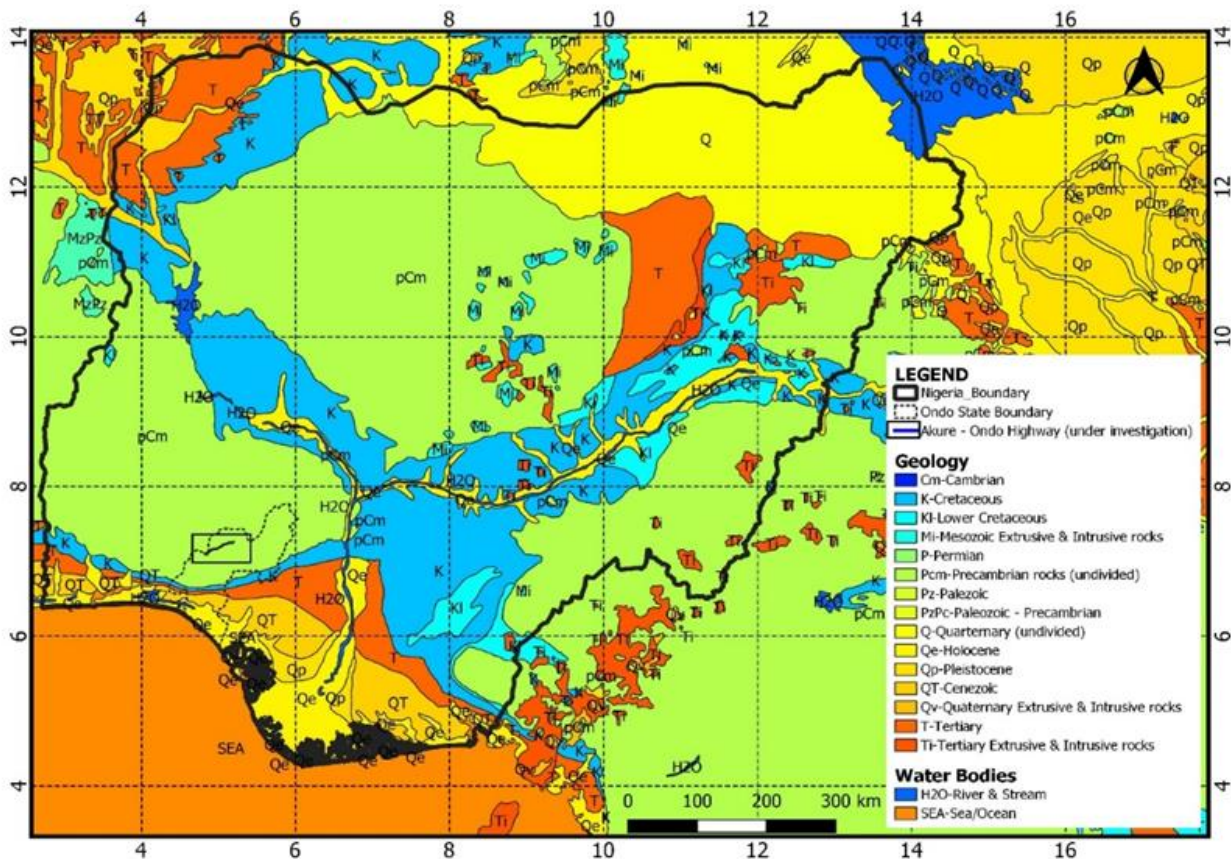


Figure 2. Geological map of Nigeria showing the highway under investigation (modified after Nigerian Geological Survey Agency [40])

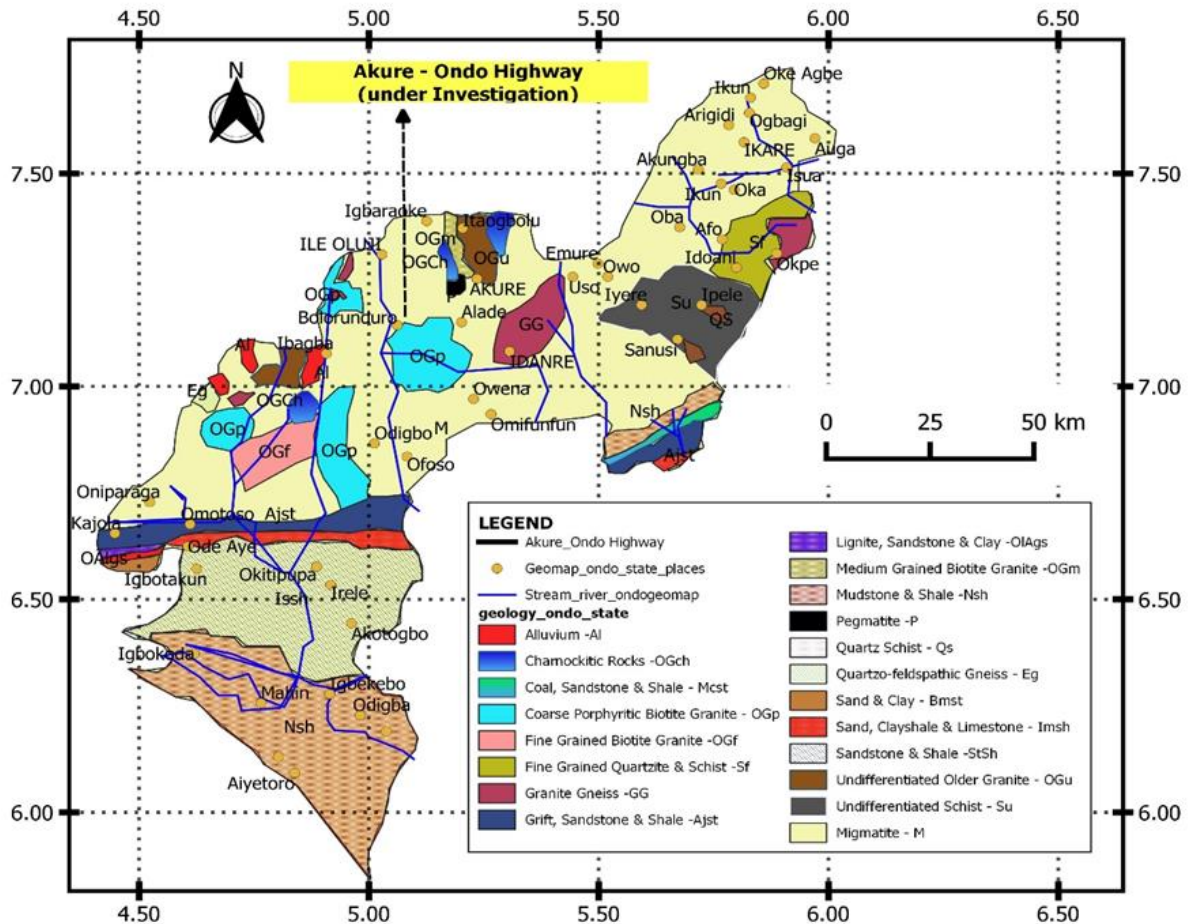


Figure 3. Geological Map of Ondo State showing the road under investigation straddling migmatite, and granite rock units (modified after NGS [41])

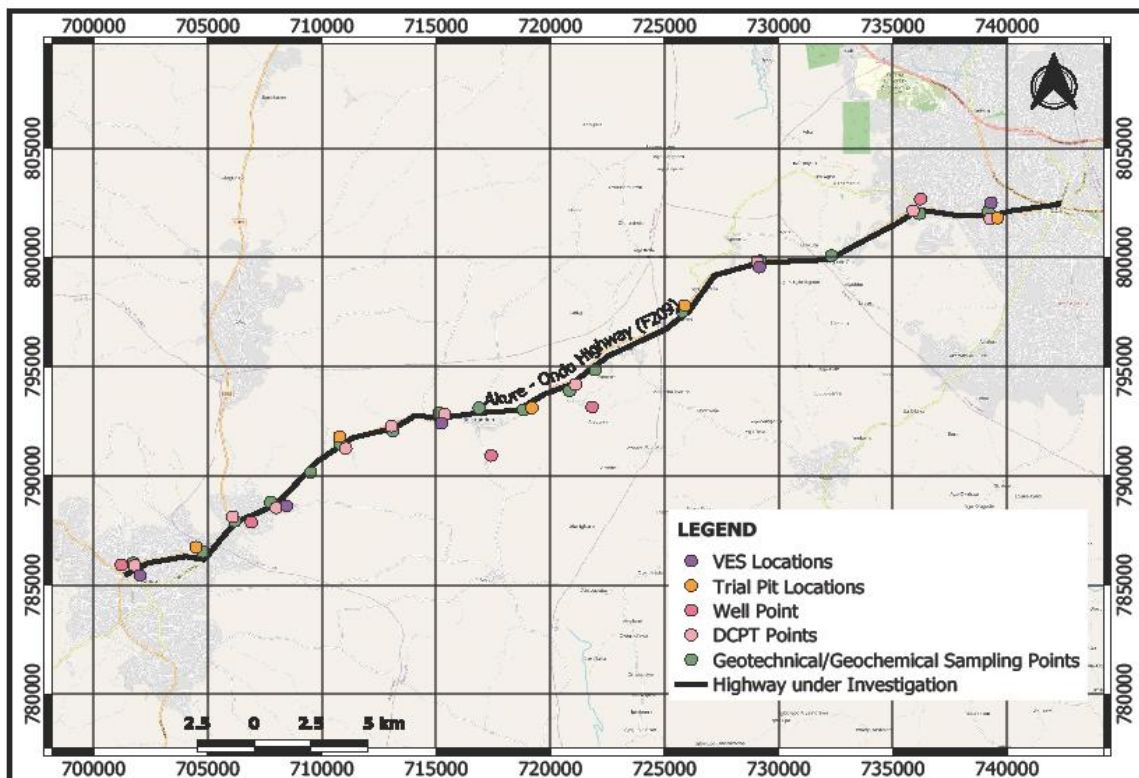


Figure 4. Data acquisition map for the study showing the geotechnical/geochemical sampling points, geophysical locations, and trial pit points

2.3. Field and laboratory procedures

The data obtained (in terms of resistivity and thickness) was plotted as a graph of apparent resistivity against half the current electrode separation. Consequently, the electrode separation at which inflection points occur in the graph gives an idea of the depth/thickness of interphases of the layers and their resistivity. The WinResist software was used for the data analysis involving curve fitting and modeling [42-43]. The result of the modeling was used to develop the geoelectric section along the highway.

The DCPT was taken along the highway at about 1.0 to 5.0 m offset away from the edge of the highway (Figure 5). The DCP is a simple mechanical device used for rapid in-situ strength determination of highway structural material, especially the subgrade and other unbound layers [44-45], and is capable of delivering 45.5 Joules of energy. It measures the penetration of a standard cone when driven by a standard force [46-47]. The DCP penetrative index in mm per blows of the standard hammer is recorded together with number of blows and depth of penetration. In this study, the standard steel cone with an angle of 60° and a diameter of 20 mm was used. The standard 8 kg hammer was also utilized which slides over a 16 mm diameter steel rod with a fall height of 575 mm that strikes the anvil to cause penetration. The test was conducted at ten (10) locations along the highway. This limited test number was due to insecurity that usually characterized failed highway. The UK DCP 3.1 software was used for the analysis and interpretation of the data collected [44]. In calculating the CBR using the Transport and Road Research Laboratory (TRL) [48] relationship, the data recorded at each of the site was corrected for moisture content using the adjustment factor in Table 1. All the test sites were numbered serially from Test No. 1 to test. No. 10.



Figure 5. DCPT Field Survey carried out along Akure – Ondo Highway at different locations

Table 1. CBR adjustment factor [44]

Surface moisture	Ratio of in-situ moisture to OMC (modified AASHTO)	Default CBR adjustment factor
Wet	1	1
Moderate	0.75	0.71
Dry	0.5	0.51
Very dry	0.25	0.37
Unknown*	-	0.5

* not assessed or difficult to assess

The strength coefficient of the test sites was calculated by the UK DCP 3.1, by converting the penetration rate to CBR value and then to strength coefficient and finally to structural number. The TRL equation was used for CBR calculation, as stated in Equation 1. The strength coefficient of the subsoil for usage as the base and subbase layers is calculated using Equation 2 (for base) and Equation 3 (for subbase).

$$\text{Log}_{10}^{(\text{CBR})} = 2.48 - 1.057 \text{Log}_{10}^{(\text{pen rate})} \quad (1)$$

$$a = 0.0001[29.14 (\text{CBR}) - 0.1977 (\text{CBR})^2 + 0.00045 (\text{CBR})^3] \quad (2)$$

$$a = 0.184 \text{Log}_{10}^{(\text{CBR})} - 0.0444 (\text{Log}_{10}^{(\text{CBR})})^2 - 0.075 \quad (3)$$

The SNG which is referred to as subgrade structural number i.e., the contribution of the subsoil has subgrade material to structural number of a pavement [44]. It is usually derived from CBR just like the base and the subbase layers. The relationship between SNG and CBR is presented in Equation 4.

$$\text{SNG} = 3.51 \text{Log}_{10}^{(\text{CBR})} - 0.85 \text{Log}_{10}^{(\text{CBR})^2} - 1.43 \quad (4)$$

The relative densities of each subsoil layering were derived using DIN 4094 [49] model (Equation 5, where n_{10} is the number of blows for every 10 cm). The resilient modulus (using [50, 51, 52] models, as shown in Equations 6 – 8 respectively) and Young modulus were obtained from each site along the highway alignment using Equation 9.

$$I_D = 0.21 + 0.230 \log n_{10} \quad (5)$$

$$M_R = 10^{3.04758 - 1.06166 \log(\text{DCPI})} \quad (6)$$

$$M_R = 235.3 \times \text{DCPI}^{-0.475} \quad (7)$$

$$M_R = 338 \times \text{DCPI}^{-0.39} \quad (8)$$

$$E_R = \frac{M_R - 12.69}{1.065} \quad (9)$$

From the results of models, important correlations and parameters modeling were obtained between M_R and E_R , M_R and CBR, DCPI and relative density (RD), soaked CBR and in-situ CBR, and CBR and RD.

Five trial pits were dug along the highway to study the ground conditions, as it gives opportunity to assess directly the weathered rocks [53-54]. The holes were dug with a digger by repeatedly dropping the tool into the ground. The depths range of the trial pits are within the upper 1.0 m, and no groundwater table was encountered. In addition, fifteen disturbed soil samples were taken at different chainage along the study highway as shown in Figure 4. The samples were collected at shallow depth of less than 1m from holes different from the trial pits. They were subjected to geotechnical tests and geochemical tests. The geotechnical tests were conducted using ASTM methods/procedures [55], and these included California Bearing Ratio (D-1883), compaction test (D-1557), particle size analysis (D-422), Atterberg limits (D-4318), moisture content (D-2216) and specific gravity (D-854; D-5550). The geochemical test was only analyzed for mineral oxides of SiO_2 , Fe_2O_3 , and Al_2O_3 using X-ray diffraction technique. Subsequently, the silica/sesquioxides (se) ratio was calculated to know the type of the soil and classified if laterite ($se < 1.33$), lateritic ($1.33 < se < 2.0$) and non-laterite ($se > 2.0$).

Traffic survey (classified volume counts) was conducted for seven days taking records of all vehicles plying the highway per day [1]. It was conducted by noting the number of various classes of vehicles that pass the count point in each direction, hence average of daily traffic was used in estimating design thickness for highway pavement.

3. Results

The summary of the Vertical Electrical Sounding (VES) was presented in Table 2, while the geoelectric section along the highway is shown in Figure 6. The curve types obtained from the highway alignment varied from three-layer curve (H) to four-layer curve (KH). The KH-curve type is the most preponderant (80 %), while H-curve constituted 20 %. Geologically, the soil underneath the pavement consists of topsoil (clay, sandy clay, and clay sand), subsoil (sandy clay, clay sand, sand, and laterite), weathered layer, fractured basement (under VES 5) and fresh basement rock (Table 3). The pit sections (Figure 7) depict five geologic units across the pavement alignment, consisting of stiff clay-sand mixture, lateritic soil, clayey hardpan, sandy clay, and clay soil. The upper 0.5 m is generally made up of laterite/stiff clay-sand mixture (trial pit 01), sandy clay/laterite (trial pit 02), sandy clay (trial pits 3 and 5) and clay (trial pit 04). The results of chemical analysis (oxides) of the major elements (SiO_2 , Fe_2O_3 , and Al_2O_3) contained in the soil samples, and silica-sesquioxide (S-S) ratio are presented in Table 4. The samples are well dominated (in descending order) by $\text{SiO}_2 - \text{Fe}_2\text{O}_3 - \text{Al}_2\text{O}_3$, ranging from 55.6 – 63.5 % (avg. 59.4

%), 17.9 – 21.4 % (avg. 19.4 %), and 15.4 – 18.8 % (avg. 17.1 %) respectively. S-S ratio of the samples ranged from 1.49 to 1.81 (avg. of 1.63).

Table 2. Summary of VES results

East	North	Elevation (m)	VES NO.	Resistivity (Ohmns-meter)					Thickness (m)				Depth (m)				Curve Type
				ρ_1	ρ_2	ρ_3	ρ_4	ρ_5	h_1	h_2	h_3	h_4	d_1	d_2	d_3	d_4	
739583	801891	341	1	45	268	55	3145	-	0.9	6.9	25.5	-	0.9	7.8	33.3	-	KH
729253	799252	335	2	141	205	98	999	-	0.8	14.2	22.6	-	0.8	15.0	37.6	-	KH
715236	792016	328	3	258	898	159	2556	-	0.6	7.9	32.3	-	0.6	8.5	40.8	-	KH
708410	788147	291	4	755	285	2528	-	-	1.2	19.1	-	-	1.2	20.3	-	-	H
702084	785007	284	5	225	623	45	884	-	0.5	1.9	29.5	-	0.5	2.4	31.9	-	KH

Table 3. Rating of subsoil competence using resistivity values

App. resistivity range (ohm-m)	Lithology	Competence rating
< 100	Clay	Incompetent
100 – 350	Sandy clay	Moderately competent
350 – 750	Clayey sand	Competent
> 750	Sand/Laterite/Crystalline Rock	Highly competent

Table 4. Result of the chemical analysis of three major mineral oxide

MA	S1	S2	S3	S4	S5	S6	S7	S8	S9	S10	S11	S12	S13	S14	S15
SiO ₂	60.7	59.8	63.5	60.2	58.7	58.9	60.5	55.6	57.2	56.6	60.8	59.5	62.4	57.8	58.2
Al ₂ O ₃	16.22	18.8	15.65	16.23	15.87	18.2	17.32	16.55	16.45	18.3	15.44	18.11	18.2	16.98	18.5
Fe ₂ O ₃	18.63	20.32	21.25	19.65	21.4	20.9	18.2	18.65	18.33	19.58	18.22	18.56	17.87	18.54	20.1
S-S ratio	1.74	1.53	1.72	1.68	1.57	1.51	1.70	1.58	1.64	1.49	1.81	1.62	1.73	1.63	1.51
ST	L	L	L	L	L	L	L	L	L	L	L	L	L	L	L

MA: Mineral oxide; ST: Soil type; L: Lateritic

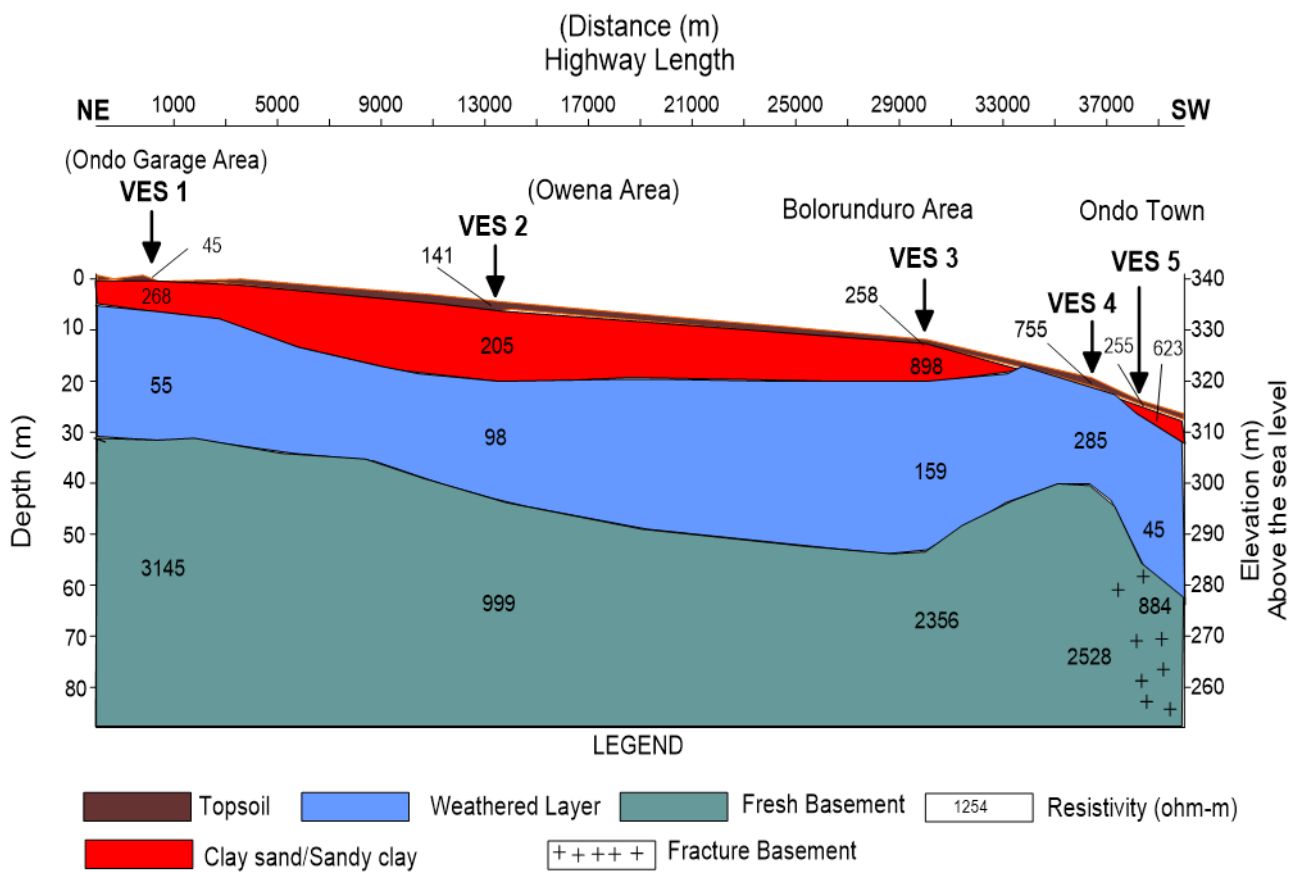


Figure 6. Goelectric Section along the highway alignment

Table 5 presents the summary of the geotechnical results. The natural moisture content varied from 13.6 to 23.3 % (avg. 12.9 %). The gravel and sand contents varied from 0 – 1.2 % (avg. 0.8 %) and 45.3 – 55.8 % (avg. 50.6 %) respectively. The % silt and clay contents ranged from 10.9 to 25.1 % (avg. 19.4 %) and 23.5 to 34.2 % (avg. 29.2 %). The % fines ranged from 43 to 54.5 (avg. 48.6). The composition of the soil is dominated (in order of magnitude) by sand, clay, and silt (SC-SM). The plasticity chart (Figure 8a) showed that the fines in the samples is dominated by clay of intermediate plasticity/compressibility, 70 % of the soil samples plotted above the A-line. In terms of clay mineralogy, the soil samples are plotted within the illite clay mineralogy group (Figure 8b). The activity ranged from 0.54 to 0.85 (avg. 0.69) signifying inactive clay type. The values of specific gravity of the

samples ranged between 2.65 – 2.75 (avg. 2.689). The liquid limit (LL) values ranged between 39.7 and 49.9 % (avg. 44.2 %), plastic limits (PL) ranged between 20.2 and 27.5 % (avg. 24.1 %) and plasticity index (PI) is between 17.1 and 23.5 % (avg. 20.1 %). The linear shrinkage (SL) ranged between 7.2 to 12.5 % (avg. 9.2 %), The maximum dry density (MDD) for the soil samples varied between 1760 and 2008 kg/m³ (1904 kg/m³) at standard proctor compaction energy while the optimum moisture content (OMC) ranged between 16.9 and 25.8 % (20.6 %). All compacted samples showed unsoaked CBR values ranging between 7 and 19 % (avg. 12 %), with corresponding in-situ values obtained from DCPT ranging from 5 to 31 % (avg. 12 %). The Group Index (GI) values obtained ranged from 4 to 9 (avg. 7).

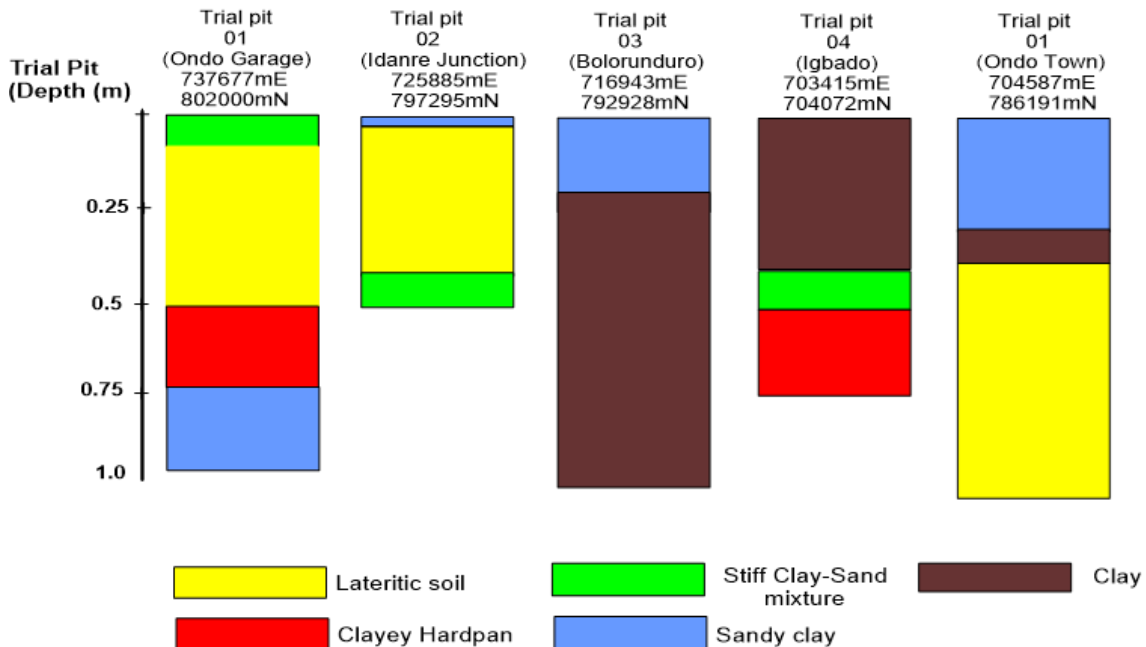


Figure 7. Trial pit of the three sites investigated along the Highway showing the columnar sections

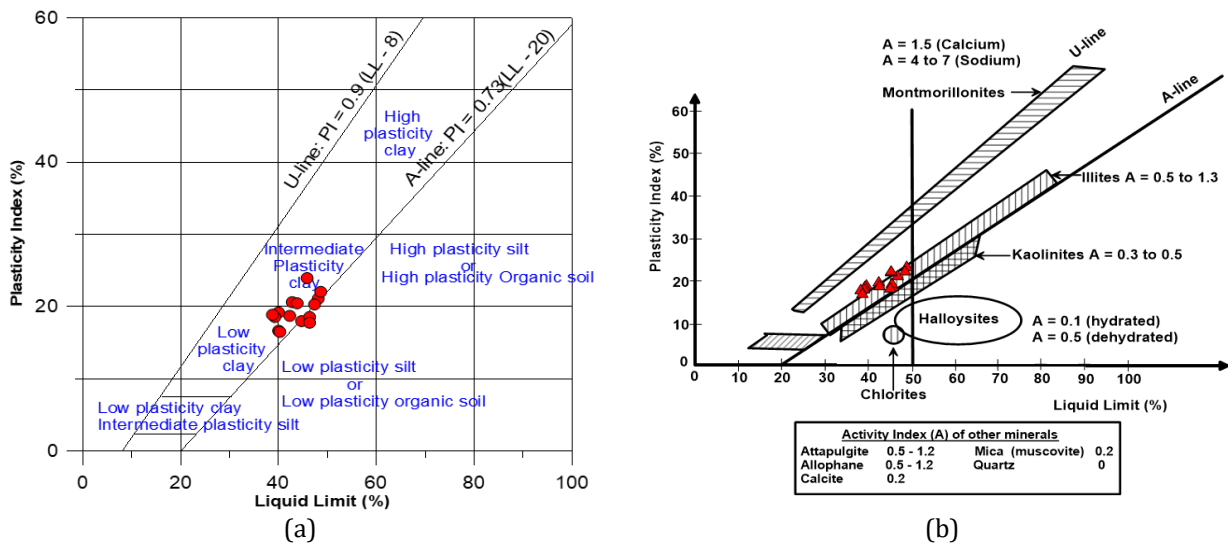


Figure 8. (a) Plasticity Chart for Fine Contents of the soil samples (b) Clay mineralogy group of the soil samples with most within/or near the illite

The result summary of the DCPT is presented in Table 6, while subsoil layering in relation to its depth and in-situ CBR are shown in Figures 9 and 10. In Table 6, the degree of penetration ranged from 942 mm (Test 3) – 997 mm (Test 2), with cumulative number of blows ranging from 27 (Test 5) to 130 (Test 3). The penetrative index or rate ranged between 1.20 mm/blow (Test 3 at penetration depth of 923 mm) – 67.0 mm/blow (Test 10 at penetration depth of 838 mm). With respect to layering, two layers (Tests 5, 6, 7, 8, and 10), three layers (Tests 1 and 4), four layers (Tests 2 and 9), and five (Test 3) were delineated. The obtained CBR ranged from 5 – 45 %. The SNG contribution of the soil as subgrade material ranged from -0.02 to 1.56.

Table 5. Summary of the geotechnical properties of the investigated soil

P	S1	S2	S3	S4	S5	S6	S7	S8	S9	S10	S11	S12	S13	S14	15
East North	739174 802141	736170 802096	732256 800048	729344 799866	725794 797545	722017 794860	720879 793904	718877 792994	616920 793131	715191 792812	713097 792038	710822 791538	709456 790127	707818 788807	706225 787943
NMC	16.5	18.4	13.6	14.9	14.2	16.8	19.4	21.3	15.4	17.9	21.2	18.4	23.3	19.8	15.7
%Gravel	0	0	1.1	1.2	0	1.2	1	1.1	0	1.2	1	1	1	1.1	1.2
%Sand	45.5	47.2	53.4	55.8	53.6	49.8	52.6	46.6	54.9	50.7	48.1	53.4	45.3	48.5	53.7
%Silt	24.4	25.1	17	18.1	17.3	18.2	17	21	10.9	19.6	20.6	17	19.9	22.9	21.6
%Clay	30.1	27.7	28.5	24.9	29.1	30.8	29.4	31.3	34.2	28.5	30.3	28.6	33.8	27.5	23.5
%Fines	54.5	52.8	45.5	43	46.4	49	46.4	52.3	45.1	48.1	50.9	45.6	53.7	50.4	45.1
SG	2.665	2.678	2.75	2.699	2.705	2.68	2.699	2.655	2.7	2.698	2.65	2.72	2.65	2.668	2.72
LL (%)	40.3	43.6	39.7	45.6	43.3	49.9	45.7	48.2	40.4	47.7	46.1	39.9	45.2	46.8	40.5
PL (%)	20.8	23.1	21.5	27	23.8	27.3	26	24.9	22	27.5	27.2	20.2	23.3	23.3	23.4
PI (%)	19.5	20.5	18.2	18.6	19.5	22.6	19.7	23.3	18.4	20.2	18.9	19.7	21.9	23.5	17.1
SL	8.9	9.5	7.8	7.2	8.1	8.5	8.0	12.3	9.6	10.1	12.5	7.9	9.9	10.2	7.7
CBR	15	13	18	19	10	8	16	7	12	14	7	12	8	9	13
(soaked)															
CBR	19	-	31	23	-	6	5	5	-	-	6	5	-	15	5
(field)															
MDD	1812	1894	1985	1928	1889	1954	1905	1785	2008	1991	1840	1999	1760	1811	2002
OMC	20.2	21.6	18.5	16.9	17.2	19.2	24.7	25.5	17.9	19.9	23.3	18.6	25.8	21.4	18.8
GI	8	8	5	4	5	8	6	9	5	7	7	5	9	8	4
GI Class	Fair	Fair	Fair	Good	Fair	Good									
Rec.															
Thickness (mm)	356	356	445	518	445	356	417	325	445	378	378	445	325	356	518
AASHTO	A-6	A-7-5	A-6	A-7-5	A-7-5	A-7-6	A-7-5	A-7-6	A-6	A-7-5	A-7-5	A-7-5	A-7-6	A-7-6	A-7-5
USCS	CL	CL	CL	ML-CL	CL	CL	ML	CL	CL	CL	ML-CL	CL	CL	CL	CL
Subgrade	Fair	Fair	Fair	Fair	Fair	Poor	Fair	Poor	Fair	Fair	Fair	Fair	Poor	Poor	Fair
Rating															
Activity	0.65	0.74	0.64	0.75	0.67	0.73	0.67	0.74	0.54	0.71	0.62	0.69	0.65	0.85	0.73
Clay Type	IA	IA	IA	N	IA	N	IA								
CM	I-M	I-M	I-M	I	I	I	I	I	I-M	I	I	I-M	I-M	I-M	I-M

P: Parameters; IA: Inactive; N: Normal; CM: Clay mineralogy

The Young modulus (E_R) and resilient modulus (M_R) was estimated from [50, 51, 52]; and the E_R varied from 10.96 – 135.8 (avg. 61.574), 65.98 – 142.62 (avg. 101.975), and 28.01 – 80.05 (avg. 52.006); the M_R ranged from 24.37 to 157.31 (avg. 78.264), 82.95 to 164.58 (avg. 121.29), and 42.52 to 97.94 (avg. 68.077) respectively. The result of the hydrogeological measurements with the static water level (SWL) measured from five open wells encountered along the highway varied from 3.5 m (migmatite) to 4.8 m (granite) with an average of 4.2 m. The hydraulic head measured with respect to sea level ranged between 315.2 m to 336.5 m (avg. 331.4 m) (Table 7). The total depth of the well investigated in close proximity to the highway alignment ranged from 7.5 – 13.5 m (avg. 10.5 m).

4. Discussion

4.1 Electrical resistivity geophysical survey

The H curve is composed of relatively high resistivity topsoil, underlain by very low resistivity subsoil/weathered layer, and bedrock; while the KH has a configuration of low resistivity overlain relatively high resistivity subsoil, followed by weathered layer and fresh or fracture or partly weathered basement. The topsoil has resistivity ranging from 45 – 755 ohm-m and thickness varying from 0.5 – 1.2 m and composed of clay, sandy clay, and clay sand (using interpretation Table 3). The range of 100 – 350 ohm-m is the most occurring signifying a predominant sandy clay composition. The subsoil delineated except under VES 4 is characterized with resistivity ranging from 205 – 898 ohm-m composing sandy clay, clay sand, sand, and laterite. The thickness of this layer ranged from 1.9 to 14.2 m (VES 2). The weathered layer is clayey and has resistivity ranging between 45 ohm-m and 159 ohm-m. The fracture basement was only observed under VES 4 with resistivity of 884 ohm-m. The fresh basement has resistivity ranging from 999 – 3145 ohm-m, depths to basement rock varied from 20.3 – 40.8 m, indicating thick weathering profile. Consequently, the topsoil and subsoil are generally composed of sandy clay/clay sand soil material, which can be regarded as fairly competent soil material to support the pavement structure. It is observed that the basement relief slopes downwardly towards the southwestern part.

4.2 Trial pits

Trial pits can be used for all soil types irrespective of texture, grain size, and mineralogy. It is the cheapest way of site exploration, and do not require any specialized equipment [15-16]. In this method a pit is manually excavated and soil is inspected in the natural condition. Therefore, the soil on which the highway is founded is dominantly sandy clay and laterite, which is a fair - good competent soil for civil engineering construction, of which highway is not in exception.

Table 6. Summary of the DCPT showing the penetrative rate, depth of penetration, and number of blows for all the ten locations along the highway

Point	Blow	Penetration (mm)	Cum. blows	Depth (mm)	Penetration rate (mm/blow)	Blow	Penetration (mm)	Cum. blows	Depth (mm)	Penetration rate (mm/blow)	Blow	Penetration (mm)	Cum. blows	Depth (mm)	Penetration rate (mm/blow)
Test 1: 739310mE; 801277mN; CH 0 + 0.001 km LHS															
1	0	30	0	0	0	0	32	0	0	0	5	19	0	0	0
2	3	125	3	95	31.67	3	131	3	99	33.0	5	91	5	72	14.40
3	3	163	6	133	12.67	3	171	6	139	13.33	5	159	10	140	13.60
4	3	205	9	175	14.0	3	215	9	183	14.67	5	199	15	216	15.20
5	3	242	12	212	12.33	3	254	12	222	13.0	5	235	20	275	11.80
6	3	275	15	245	11.0	3	289	15	257	11.67	5	294	25	312	7.40
7	3	302	18	272	9.0	3	323	18	291	11.33	5	331	30	336	4.80
8	5	342	23	312	8.0	5	357	23	325	6.80	5	355	35	361	5.0
9	5	371	28	341	5.80	5	390	28	358	6.60	5	380	40	393	6.40
10	5	400	33	370	5.80	5	424	33	392	6.80	5	412	45	431	7.60
11	5	449	38	419	9.80	5	472	38	440	9.60	5	450	50	463	6.40
12	5	510	43	480	12.20	5	536	43	504	12.80	5	482	55	476	2.60
13	5	575	48	545	13.0	5	604	48	572	13.60	5	495	60	503	5.40
14	5	649	53	619	14.80	5	683	53	651	15.80	5	522	65	544	8.20
15	5	730	58	700	16.20	5	788	58	756	21.0	5	563	70	592	9.60
16	5	790	63	760	12.0	5	840	63	808	10.40	5	611	75	633	8.20
17	5	831	68	801	8.20	5	882	68	850	8.40	5	652	80	683	10.0
18	5	882	73	852	10.20	5	935	73	903	10.60	5	702	85	726	8.60
19	5	946	78	916	12.80	5	997	78	965	12.40	5	745	90	793	13.40
20	-	-	-	-	-	-	-	-	-	-	5	812	95	826	6.60
21	-	-	-	-	-	-	-	-	-	-	5	845	100	846	4.0
22	-	-	-	-	-	-	-	-	-	-	5	865	105	880	6.80
23	-	-	-	-	-	-	-	-	-	-	5	899	110	896	3.20
24	-	-	-	-	-	-	-	-	-	-	5	915	115	905	1.80
25	-	-	-	-	-	-	-	-	-	-	5	924	120	917	2.40
26	-	-	-	-	-	-	-	-	-	-	5	936	125	923	1.20
27	-	-	-	-	-	-	-	-	-	-	5	942	130	-	-
Test 2: 735988mE; 801914mN; CH 0 + 5.1 km RHS															
Test 3: 729071mE; 799320mN; CH 0 + 7.2 km RHS															
Test 4: 7212891mE; 793654mN; CH 0 + 12.5 km LHS															
1	5	20	0	0	0	0	34	0	0	0	0	0	0	0	0
2	5	89	5	69	13.80	3	189	3	154	51.33	3	180	3	146	48.67
3	5	155	10	135	13.20	3	278	6	243	29.67	3	264	6	230	28.0
4	5	205	15	185	10.0	3	351	9	316	24.33	3	333	9	299	23.0
5	5	228	20	208	4.60	3	423	12	388	24.0	3	402	12	368	23.0
6	5	285	25	265	11.40	3	480	15	445	19.0	3	456	15	422	18.0
7	5	321	30	301	7.20	3	538	18	503	19.33	3	504	18	470	16.0
8	5	344	35	324	4.60	3	670	21	635	44.0	3	636	21	602	44.0
9	5	369	40	349	5.0	3	851	24	816	60.33	3	801	24	767	55.0
10	5	401	45	381	6.40	3	961	27	926	36.67	3	912	27	878	37.0
11	5	437	50	417	7.20	-	-	-	-	-	3	950	30	916	12.67
12	5	466	55	446	5.80	-	-	-	-	-	-	-	-	-	-
13	5	485	60	465	3.80	-	-	-	-	-	-	-	-	-	-
14	5	502	65	482	3.40	-	-	-	-	-	-	-	-	-	-
15	5	539	70	519	7.40	-	-	-	-	-	-	-	-	-	-
16	5	602	75	582	12.60	-	-	-	-	-	-	-	-	-	-
17	5	666	80	646	12.80	-	-	-	-	-	-	-	-	-	-
18	5	743	85	723	15.40	-	-	-	-	-	-	-	-	-	-
19	5	792	90	772	9.80	-	-	-	-	-	-	-	-	-	-
20	5	852	95	832	12.0	-	-	-	-	-	-	-	-	-	-
21	5	889	100	869	7.40	-	-	-	-	-	-	-	-	-	-
22	5	923	105	903	6.80	-	-	-	-	-	-	-	-	-	-
23	5	966	110	946	8.60	-	-	-	-	-	-	-	-	-	-
Test 5: 715464mE; 792243mN; CH 0+ 15.0 km RHS															
Test 6: 713143mE; 791788mN; CH 0 + 17.2 km LRS															
Test 7: 711140mE; 790741mN; CH 0 + 24.3 km LHS															
1	0	0	0	0	0	3	30	0	0	0	3	30	0	0	0
2	3	36	3	146	50.33	3	118	3	88	29.33	3	84	3	54	18.0
3	3	187	6	230	28.33	3	165	6	135	15.67	3	132	6	102	16.0
4	3	272	9	299	23.67	3	219	9	189	18.0	3	179	9	149	15.67
5	3	343	12	368	24.0	3	305	12	275	28.67	3	268	12	238	29.67
6	3	415	15	422	18.33	3	390	15	360	28.33	3	349	15	319	27.0
7	3	470	18	470	19.0	3	425	18	395	11.67	3	371	18	341	7.33
8	3	527	21	602	43.33	3	505	21	475	26.67	3	453	21	423	27.33
9	3	657	24	767	59.0	3	645	24	615	46.67	3	605	24	575	50.67
10	3	834	27	878	38.67	3	788	27	758	47.67	3	747	27	717	47.33
11	3	952	30	916	30.53	3	881	30	851	31.0	3	854	30	824	35.67
12	-	-	-	-	-	3	952	33	922	23.67	3	933	33	903	26.33
13	-	-	-	-	-	-	-	-	-	-	3	955	36	922	6.33
Test 8: 708000mE; 787965mN; CH 0 + 36.0 km LHS															
Test 9: 706180mE; 787419mN; CH 0 + 40.1 km RHS															
Test 10: 702038mE; 785326mN; CH 0 + 42.0 km RHS															
1	3	29	0	0	0										
2	3	129	3	100	33.33										
3	3	181	6	152	17.33										
4	3	241	9	212	20.0										
5	3	336	12	307	31.67										
6	3	351	15	322	5.0										
7	3	468	18	439	39.0										
8	3	556	21	527	29.33										
9	3	666	24	637	36.67										
10	3	867	27	838	67.0										
11	3	968	30	939	33.67										

Table 7. Hydrogeological measurement of wells in close proximity to the pavement

East	North	Well No	Elevation (m)	Total Depth	SWL	Water Column (m)	Hydraulic Head (m)	Geology
736170	802119	W-1	345	12.5	4.5	8.0	340.5	Migmatite
721971	792744	W-2	351	7.8	3.8	4.0	347.2	Migmatite
717602	790514	W-3	322	7.5	4.2	3.3	317.8	Granite
706908	787419	W-4	320	11.2	4.8	6.4	315.2	Granite
701310	785644	W-5	340	13.5	3.5	10.0	336.5	Quartzite

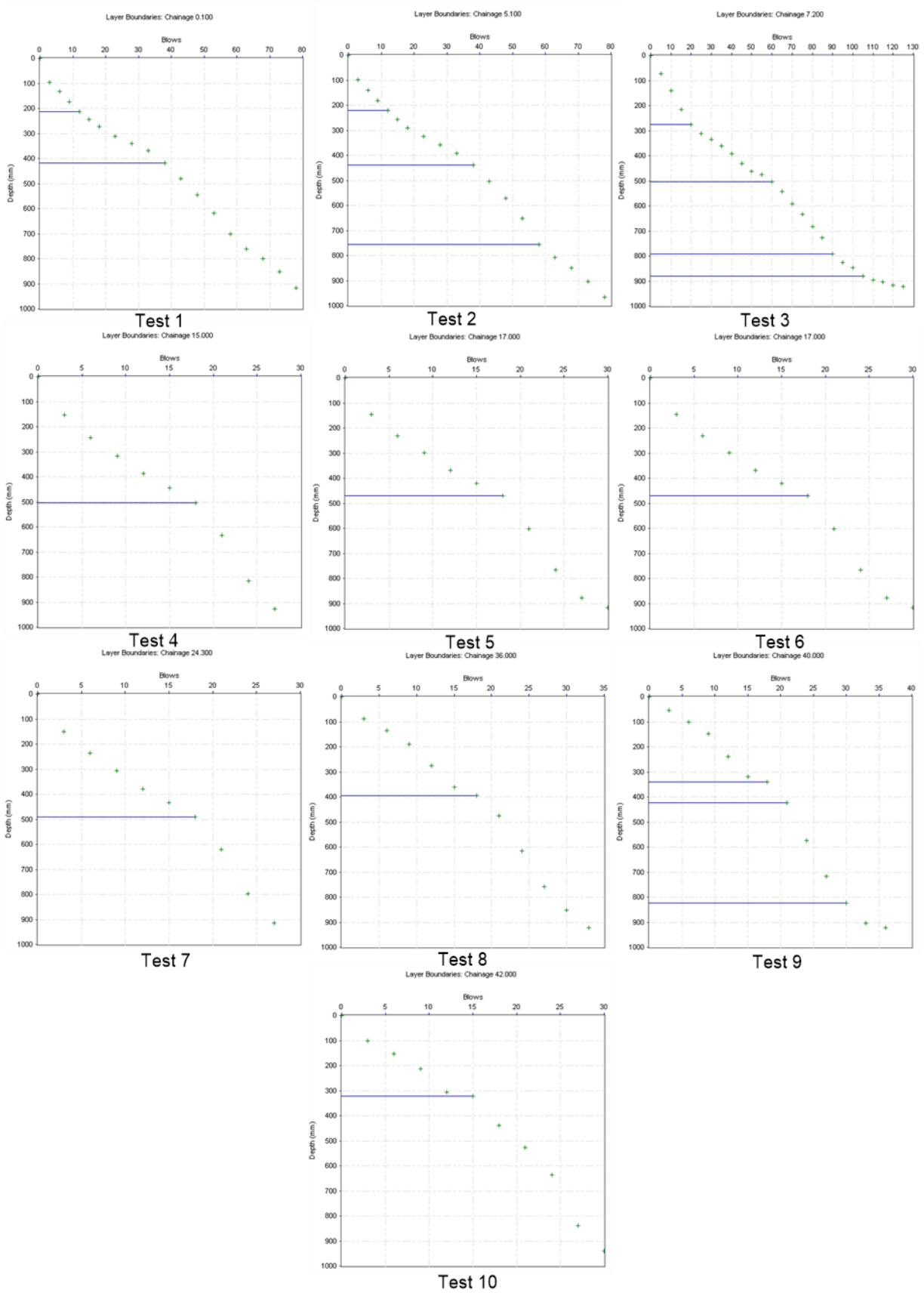


Figure 9. The plot of cumulative blows against depth at test points 1 – 10 showing the layering within the upper 1.0 m

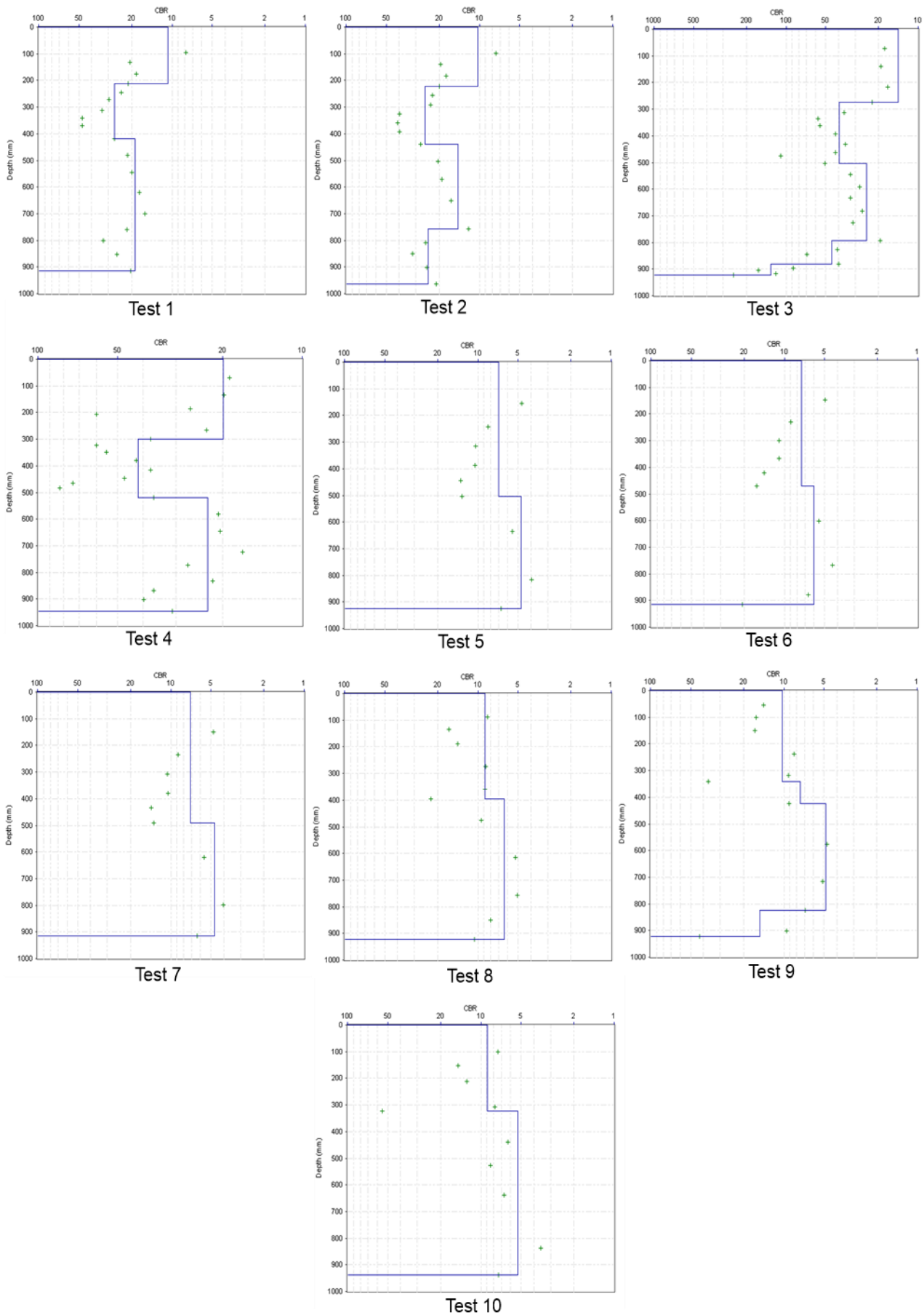


Figure 10. The plot of CBR against depth at test points 1 – 10, showing the CBR of the layers

4.3 Geochemical analysis

The stability and serviceability performance depends on the mineralogical make-up of the soil [15]. Accordingly, soils with S-S ratio between 1.33 and 2.0 are categorized as lateritic soil type. This corroborates the lateritic soil observed from the trial pit sections.

4.4 Geotechnical analysis

The range of Natural Moisture Content (NMC) is above 5 – 15 % acceptable range favorable for civil engineering uses or construction, but if the average value is considered, the soil still satisfied the requirement. Grain size analysis can be used to characterize the subsoil material for engineering foundation, which can serve as a guide to the engineering performance of the soil type and also provides a means by which soils can be identified quickly. The amount of % fines recorded is more than 35 % specification of Federal Ministry of Works and Housing [56] for highway subgrade. The soil samples plotted within the illite clay mineralogy group (Figure 8b). Illite has a structure similar to montmorillonite, however in illite the interlayers are bonded together with a potassium ion linkage, making it to have relatively less attraction for water [15-16]. Therefore, it is expected that the soil will exhibit more of illite characteristics.

The specific gravity (SG) is closely related with soil's mineralogy and/or chemical contents; the higher SG, the higher the degree of laterization. In addition, the larger the clay fraction and alumina contents, the lower is the SG. The standard range of value of specific gravity of soils for civil engineering construction lies between 2.60 and 2.80, hence the obtained values are considered normal for civil engineering construction; hence the soils are competent. Specific gravity is known to correlate with mechanical strength of soil and may be used as a basis for selecting suitable highway pavement construction materials particularly when used with other pavement construction materials.

The Federal Ministry of Works and Housing (FMWH) [56] recommends LL of 50% (max.), PI of 20% as (max.), plastic limit of 30 % (max.) and % fines of 35 maximum for highway subgrade soil. Soil with high LL, PL, and PI are usually characterized with low bearing pressure. Hence the soils satisfied these requirements as subgrade material. The obtained values of linear shrinkage (SL) signified a moderate swelling potential, even though SL greater than 8.0 tends to be active, of critical swelling potential.

Compaction is concerned with relationships between moisture content, applied effort and density. Compaction is undertaken on roads to enhance the mass density and hence the strength, rigidity and durability of placed materials. In the laboratory compaction testing is undertaken to predict moisture density responses of a material to applied effort and to provide a reference with which to control on-site compaction during construction [16], [19]. An important part of the grading of the site often includes the compaction of fill. All the soil samples have high MDD at moderately low OMC.

The California Bearing Ratio (CBR) is an empirical test employed in road engineering as an index of compacted material strength and rigidity, corresponding to a defined level of compaction [13]. The Federal Ministry of Works and Housing [56] recommends a California Bearing Ratio of greater than 10% for subgrade materials. Therefore, using Table 8, the soils are rated as fair (based on average value) in terms of pavement subgrade material. The obtained average GI value corresponds to fair subgrade soil. The result shows that the California Bearing Ratio values of the soils both in-situ and laboratory satisfied the 10 % minimum specification. Using Table 9, the soil can be regarded as subgrade soil with medium strength classification. Based on the GI and CBR values, and the traffic count carried out which placed the highway as Class-E, the recommended thickness of the basement should range from 325 mm (good segment) to 518 mm (for weak segment) (avg. 404 mm) as shown in Figure 11. This recommended thickness is far above the measurement carried out in the field along the highway structure which is 192 – 316 mm (Figure 12). This implies that the highway is thickness deficit, which may cause the failure of the pavement structure.

4.5 In-situ DCPT

From the CPT result, all the tests are characterized with low - high cumulative number of blows in the upper 1 m investigated, signifying a loose - medium/dense consistencies of relative densities of 0.320 to 0.509 (Table 10). However notable weak test points including Tests 5, 8, and 10 are characterized with loose soil material, while test points 1 – 4, and 9 are made up of medium soil. The most competent layers in terms of the obtained CBR are generally between 212 mm (Test 1) to 824 mm (Test 9). The estimated relative densities (RD) give consistencies of the soil either as very dense, dense, medium, loose or very loose, however it showed layering not totally consistent with those observed from DCPI. These range of values are fairly above 0.5 SNG strength coefficient for subgrade pavement layer. Thus, the depth range of 900 – 1000 mm are characterized with soils of SNG greater than 0.5. Consequently, relating the CBR and SNG, the appropriate depths for Test points 1 - 4 are 212 mm, 756 mm, 793 mm, and 301 mm respectively; while for Test points 5 – 8 and 10, the respective depths of 503 mm, 470 mm, 491 mm, 395 mm, and 322 mm are the best. The strength coefficient of the soils as subbase and base are less

than 0.5 and ranged from 0.03 – 0.12, and 0.01 – 0.14, with Structural Number (SN)/modified Structural Number (SNC) and adjusted Structural Number (SNP) ranging from 1.44 to 3.53 and 1.14 to 2.24; and 0.61 to 2.45 and 0.61 to 2.45 respectively. From the values, the strength coefficient is generally low for subbase and base material. Resilient modulus (M_R) is a measure of subgrade material stiffness. It is a means of estimating modulus of elasticity (E_R) of rapidly applied loads as against slowly applied load used for E_R [26, 28]. Lockwood *et al.* [50] and George and Uddin [52] showed closely overlapping values, while Jianzhou *et al.* [51] showed a wide variation (Table 11) in the values of E_R and M_R .

Table 8. Summary of the CBR results in relation to strength coefficient of the soils as subgrade, subbase, and base material

Test No.	Test layer No.	CBR (%)	Thickness (mm)	Depth (mm)	Subgrade SNG	Position	Strength coefficient	Pavement Strength/Layer contribution			Position	Strength coefficient	Pavement Strength/Layer contribution			
								SN	SNC	SNP			SN	SNC	SNP	
1	1	11	212	212	0.45	SB	0.07	3.07	3.07	1.95	Base	0.03	1.72	1.72	1.72	
	2	27	207	419	1.16	SB	0.10				Base					0.07
	3	19	497	916	0.88	SB	0.09				Base					0.05
2	1	10	222	222	0.38	SB	0.07	3.16	3.16	1.92	Base	0.03	1.75	1.75	1.75	
	2	26	218	440	1.13	SB	0.10				Base					0.06
	3	14	316	756	0.64	SB	0.08				Base					0.04
	4	24	209	965	1.07	SB	0.09				Base					0.06
3	1	14	275	275	0.64	SB	0.08	3.44	3.44	2.14	Base	0.04	2.45	2.45	2.45	
	2	39	228	503	1.45	SB	0.11				Base					0.09
	3	25	290	793	1.10	SB	0.10				Base					0.06
	4	45	87	880	1.56	SB	0.11				Base					0.10
	5	31	43	923	1.27	SB	0.12				Base					0.14
4	1	20	301	301	0.92	SB	0.09	3.53	3.53	2.24	Base	0.05	2.33	2.33	2.33	
	2	42	218	519	1.51	SB	0.11				Base					0.09
	3	23	427	946	1.03	SB	0.09				Base					0.06
5	1	7	503	503	0.10	SB	0.05	1.45	1.45	1.45	Base	0.02	0.61	0.61	0.61	
	2	5	423	926	-0.16	SB	0.03				Base					0.01
6	1	7	470	470	0.10	SB	0.05	1.69	1.69	1.15	Base	0.02	0.68	0.68	0.68	
	2	6	446	916	-0.02	SB	0.04				Base					0.02
7	1	7	491	491	0.10	SB	0.05	1.44	1.44	1.44	Base	0.02	0.61	0.61	0.61	
	2	5	423	914	-0.16	SB	0.03				Base					0.01
8	1	9	395	395	0.30	SB	0.06	1.83	1.83	1.26	Base	0.02	0.74	0.74	0.74	
	2	6	527	922	-0.02	SB	0.04				Base					0.02
9	1	10	341	341	0.38	SB	0.07	1.84	1.84	1.28	Base	0.03	0.81	0.81	0.81	
	2	8	82	423	0.20	SB	0.05				Base					0.02
	3	5	401	824	-0.16	SB	0.03				Base					0.01
	4	15	98	922	0.70	SB	0.08				Base					0.04
10	1	9	322	322	0.30	SB	0.06	1.61	1.61	1.14	Base	0.02	0.67	0.67	0.67	
	2	5	617	939	-0.16	SB	0.04				Base					0.01

SB: Sub-Base

Table 9. Subgrade strength classification for the studied highway [19]

Soaked CBR	Strength classification	Comments
< 1%	Extremely weak	Geotextile reinforcement and separation layer with a working platform typically required
1 % - 2 %	Very weak	Geotextile reinforcement and/or separation layer and/or a working platform typically required
2 % - 3 %	Weak	Geotextile separation layer and/or a working platform typically required
3 % - 10 %	Medium	Good subgrades to sub-base quality material
10 % - 30 %	Strong	
>30%	Extremely strong	Sub-base to base quality material

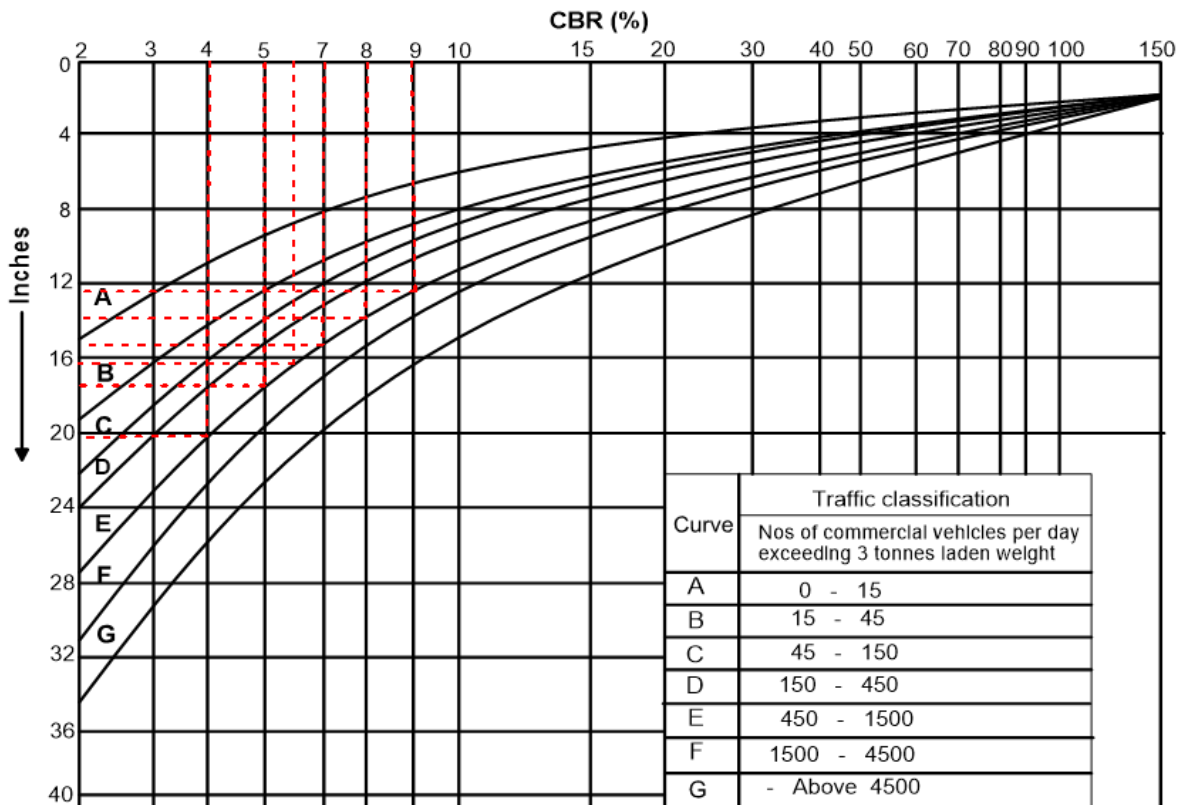


Figure 11. The CBR Chart adopted for the determination of the recommended thickness across the highway alignment



Figure 12. Sections of the Highway Structure Exposed along the highway edge/shoulder from which existing design thickness was measured (a) weak subgrade segment (b) good subgrade segment

Table 10. DCPT results showing relative densities per every 10 cm, their penetrative rate, and the consistencies of the soil

Test 1									
Depth (cm)	10	20	30	40	50	60	70	80	90
Blows per 10 cm	3	9	9	6	6	3	6	6	6
Relative Density	0.320	0.429	0.429	0.389	0.389	0.320	0.389	0.389	0.389
Soil Consistency	Loose	Medium	Medium	Medium	Medium	Loose	Medium	Medium	Medium
PR (mm/blow)	31.67	14.0	9.0	5.80	12.0	-	-	-	10.20
Test 2									
Depth (cm)	10	20	30	40	50	60	70	80	90
Blows per 10 cm	6	9	9	6	3	6	3	6	6
Relative Density	0.389	0.429	0.429	0.389	0.320	0.389	0.320	0.389	0.389
Soil Consistency	Medium	Medium	Medium	Medium	Loose	Medium	Loose	Medium	Medium
PR (mm/blow)	33.0	-	-	-	12.8	13.6	-	10.4	10.6
Test 3									
Depth (cm)	10	20	30	40	50	60	70	80	90
Blows per 10 cm	10	10	15	15	10	10	10	20	20
Relative Density	0.440	0.440	0.481	0.481	0.440	0.440	0.440	0.509	0.509
Soil Consistency	Medium	Stiff	Stiff						
PR (mm/blow)	14.4	15.2	-	7.6	5.4	-	8.6	-	-
Test 4									
Depth (cm)	10	20	30	40	50	60	70	80	90
Blows per 10 cm	5	15	15	20	10	10	10	10	10
Relative Density	0.371	0.481	0.481	0.509	0.440	0.440	0.440	0.440	0.440
Soil Consistency	Medium	Medium	Medium	Stiff	Medium	Medium	Medium	Medium	Medium
PR (mm/blow)	-	10.0	-	-	-	12.6	9.8	-	-
Test 5									
Depth (cm)	10	20	30	40	50	60	70	80	90
Blows per 10 cm	3	3	3	3	3	3	3	3	3
Relative Density	0.320	0.320	0.320	0.320	0.320	0.320	0.320	0.320	0.320
Soil Consistency	Loose								
PR (mm/blow)	-	51.33	-	24.33	19.33	-	-	-	-
Test 6									
Depth (cm)	10	20	30	40	50	60	70	80	90
Blows per 10 cm	3	3	3	3	3	3	3	3	3
Relative Density	0.320	0.320	0.320	0.320	0.320	0.320	0.320	0.320	0.320
Soil Consistency	Loose								
PR (mm/blow)	-	-	-	23.0	16.0	-	55.0	-	37.0
Test 7									
Depth (cm)	10	20	30	40	50	60	70	80	90
Blows per 10 cm	3	3	3	3	3	3	3	3	3
Relative Density	0.320	0.320	0.320	0.320	0.320	0.320	0.320	0.320	0.320
Soil Consistency	Loose								
PR (mm/blow)	-	28.33	-	18.33	43.33	-	-	-	30.53
Test 8									
Depth (cm)	10	20	30	40	50	60	70	80	90
Blows per 10 cm	3	3	3	3	3	3	3	3	3
Relative Density	0.320	0.320	0.320	0.320	0.320	0.320	0.320	0.320	0.320
Soil Consistency	Loose								
PR (mm/blow)	-	18.0	28.67	28.33	36.67	-	-	-	31.0
Test 9									
Depth (cm)	10	20	30	40	50	60	70	80	90
Blows per 10 cm	3	6	6	3	3	3	3	3	6
Relative Density	0.320	0.389	0.389	0.320	0.320	0.320	0.320	0.320	0.389
Soil Consistency	Loose	Medium	Medium	Loose	Loose	Loose	Loose	Loose	Medium
PR (mm/blow)	-	16.0	-	-	-	50.67	-	-	-
Test 10									
Depth (cm)	10	20	30	40	50	60	70	80	90
Blows per 10 cm	6	3	6	3	3	3	3	3	3
Relative Density	0.389	0.320	0.389	0.320	0.320	0.320	0.320	0.320	0.320
Soil Consistency	Medium	Loose	Medium	Loose	Loose	Loose	Loose	Loose	Loose
PR (mm/blow)	33.33	-	-	-	-	-	-	-	33.67

PR: Penetration rate

Table 11. Summary of the Modulus of Elasticity and Resilient Modulus at every Chainage where samples were taken

Test No.	Chainage along Highway	In situ CBR	Subgrade SNG	Lockwood et al. [50]	Jianzhou et al. [51]	George and Uddin [52]	Lockwood et al. [50]	Jianzhou et al. [51]	George and Uddin [52]
1	CH. 0 + 0.001 LHS	19	0.88	58.03	105.51	53.90	74.49	125.06	70.10
2	CH. 0 + 5.1 RHS	24	1.07	60.43	106.97	54.90	77.04	126.61	71.16
3	CH. 0 + 7.2 RHS	45	1.56	124.98	138.36	76.97	145.79	160.04	94.66
4	CH. 0 + 12.5 LHS	42	1.51	113.23	133.49	73.47	133.28	154.85	90.94
5	CH. 0 + 15.0 RHS	5	-0.16	10.96	65.98	28.01	24.37	82.95	42.52
6	CH. 0 + 17.1 RHS	6	-0.02	58.79	105.98	54.22	75.30	125.55	70.44
7	CH. 0 + 24.3 LHS	5	-0.16	15.88	71.75	31.64	29.60	89.10	46.38
8	CH. 0 + 36.0 LHS	6	-0.02	24.50	80.48	37.24	38.78	98.40	52.35
9	CH. 0 + 40.0 RHS	15	0.70	135.80	142.62	80.05	157.31	164.58	97.94
10	CH. 0 + 42.0 RHS	5	-0.16	13.14	68.61	29.66	26.68	85.76	44.28

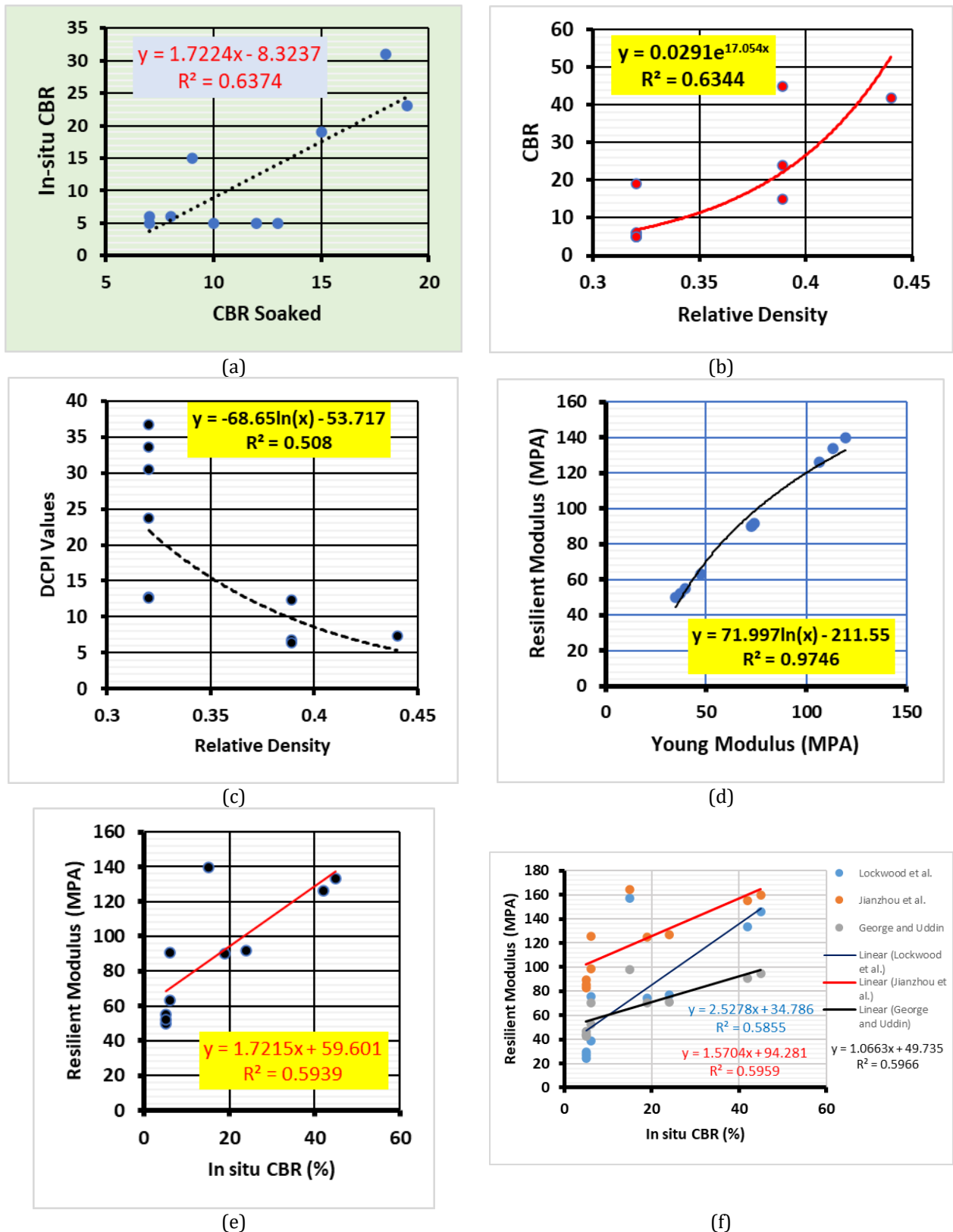


Figure 13. Regression models for (a) CBR_{lab} and in-situ CBR (b) RD and in-situ CBR (c) RD and DCPI (d) E_R and M_R (e) in-situ CBR and M_R (f) in-situ and M_R for Lockwood et al. [50], Jianzhou et al. [51], and George and Uddin [52]

4.6 Parameters modeling and correlations

The obtained soaked CBR from the laboratory was correlated with in-situ CBR obtained from processing of DCPT data, the plot gives strong positive correlation coefficient (R^2) of 0.6374 (Figure 13a), and linear regression model (Equation 10).

$$\text{CBR (in-situ)} = 1.7224x - 8.3237 \quad (10)$$

In this relationship, $x = \text{CBR (soaked)}$

The relative density (RD) values obtained from “DIN 4094” equation was plotted against in-situ CBR (Figure 13b) and DCPI (Figure 13c). This gives a regression model of Equations 11 and 12, with strong positive correlations (R^2) of 0.715 and 0.508 respectively.

$$\text{CBR (in-situ)} = 0.0291e17.054x \quad (11)$$

$$\text{DCPI} = -68.65\ln(x) - 53.717 \quad (12)$$

In these relationships, $x = \text{relative density}$

The relationship between E_R derived from “DIN 4094” and average M_R calculated from expressions proposed by [50, 51, 52] is shown by the regression model in Equation 13, with R^2 of 0.9746 (Figure 13d).

$$M_R = 71.997 \ln(x) - 211.55 \quad (13)$$

Where x is modulus of elasticity.

The correlation between in-situ CBR and average M_R derived from the expressions of [50, 51, 52] gave Equation 14, with positive correlation coefficient of 0.5939 (Figure 13e); while the plots of the in-situ CBR against each of these authors [50, 51, 52] give R^2 of 0.5855, 0.5959, and 0.5966 (Figure 13f). All the models follow the same trend. The variation in the coefficients is marginal as all showed strong positive correlations. The model expressions for these relationships are presented in Equations 15 – 17.

$$M_R = 1.7215x + 59.601 \quad (14)$$

$$M_R = 2.5278x + 34.786 \quad (15)$$

$$M_R = 1.5704x + 94.281 \quad (16)$$

$$M_R = 1.0663x + 49.735 \quad (17)$$

4.7 Hydrogeological Measurement

Consequently, the static water level (SWL) in the area is moderately low, therefore may not seriously affect the subgrade/foundation layer. However excessive cut into the subsoil during reconstruction/rehabilitation can lead to high water level situation which could compromise the integrity of the pavement structures.

5. Conclusion

The study investigated the reasons for the relative stability of Akure – Owo which is a segment of F-209 East – West Road. The study utilized combined geophysical, geochemical, hydrogeological, and geotechnical methods in probing the soil competence. Investigation showed that the subgrade is sandy clay, sand and laterite. The S-S ratio is between 1.33 and 2.0 and categorized as lateritic soil type, while the clay mineralogy group is illite. All the geotechnical properties of the soil are fair/good except the value of %fines which is above 35% maximum, however the activity of the soil showed that they are inactive. The GI of the samples have an average value of 7 corresponding to fair subgrade soil. The result showed that the California Bearing Ratio values of the soils both in-situ and laboratory have an average of 12 % and satisfied the 10 % minimum specification. Thus, based on the GI and CBR values, the recommended thickness of the basement should range from 325 mm (good segment) to 518 mm (for weak segment) (avg. 404 mm). This recommended thickness is far above the measurement of 192 – 316 mm carried out in the field along the highway structure. This implies that the highway is thickness deficit, which may likely cause the failure of the pavement structure in a distant time. In the upper 1.0 m, the SNG coefficient for subgrade soil is higher than 0.5. The strength coefficient of the soil as subbase and base is less than 0.5. The Static water level (SWL) measured from five open wells may not seriously threaten the subgrade/foundation layer. The regression models of all parameters gave strong positive correlations for all the parameters correlated: soaked CBR and in-situ CBR, E_R and M_R , in-situ CBR and M_R , RD and DCPI, and RD and in-situ CBR

It can be concluded that the relative stability of the highway was due to its good engineering properties. However imminent failure is still expected due deficit in the design thickness and lack of drainage facility along the highway’s shoulder/embankment. The haulage activities along the highway have increased tremendously of recent, and that will definitely affect the stability of the structure since it’s already thickness deficient.

Acknowledgement

Special appreciation to all students of Civil Engineering Technology Department for the assistance rendered during data acquisition, especially 2021-2022 Higher National Diploma II (HND II) students.

Funding

This research received no external funding.

Author contributions

Olumuyiwa Olusola Falowo: Conceptualization, Methodology, Software, Field Study, Visualization, Editing, Data Curation and Analysis. **Abayomi Solomon Daramola:** Data interpretation, Writing-Original draft preparation, Writing-Reviewing, and Proof-reading

Conflicts of interest

The authors declare no conflicts of interest.

References

1. Kadiyali, L. R., & Lal, N. B. (2005). Principles and Practices of Highway Engineering:(Including Expressways and Airport Engineering). Khanna Publishers.
2. Amosun, J. O., Olayanju, G. M., Sanuade, O. A., & Fagbemigun, T. (2018). Preliminary geophysical investigation for road construction using integrated methods. *Materials and Geoenvironment*, 65(4), 199-206.
3. Emmanuel, U.O., Ogonnaya, I. & Uche, U.B. (2021). An investigation into the cause of road failure along Sagamu-Papalanto highway southwestern Nigeria. *Geoenvironmental Disasters*, 8,3. <https://doi.org/10.1186/s40677-020-00174-8>
4. Owoseni, J. O., & Atigro, E. O. (2019). Engineering geological investigation of highway pavement failure in basement complex terrain of southwestern Nigeria. *International Journal of Engineering Science and Invention*, 8, (6), 1, 14-22
5. Okigbo, N. (2012). Causes of highway failures in Nigeria. *International Journal of Engineering Science and Technology*, 4(11), 4695-4703.
6. Obaje, S. O. (2017). Appraisal of Pavement Failures on Ado-Ekiti-Ogbagi Road, South-Western Nigeria. *International Journal of Geology and Earth Sciences*, 3(2), 1-9.
7. Ilori, A. O. (2015). Geotechnical characterization of a highway route alignment with light weight penetrometer (LRS 10), in southeastern Nigeria. *International Journal of Geo-Engineering*, 6, 7, 1-28. <https://doi.org/10.1186/s40703-015-0007-2>
8. Akintayo, F. O., & Osasona, T. D. (2022). Design of Rigid Pavement for Oke- Omi Road, Ibadan, Nigeria. *FUOYE Journal of Engineering and Technology*, 7(3), 382-388
9. Adetoro, A. E., & Abe, O. E. (2018). Assessment of Engineering Properties of Ado-Ekiti to Ikere-Ekiti Road Soil, Southwestern Nigeria. *World Wide Journal of Multidisciplinary Research and Development*, 4(6), 191-195.
10. Aderemi, F. L., & Adeola, R. O. (2021). Geophysical Investigation of Causes of Road Failure along Abadina Community Road, University of Ibadan, Nigeria. *Journal of Research in Environmental and Earth Sciences*, 7(1), 1-5.
11. Ekwulo, E. O., & Eme, D. B. (2009). Fatigue and rutting strain analysis of flexible pavements designed using CBR methods. *African Journal of Environmental Science and Technology*, 3(12), 412-421
12. Falowo, O. O., & Dayo, D. S. (2020). Geoenvironmental Assessment of Subgrade Highway Structural Material along Ijebu Owo – Ipele Pavement Southwestern Nigeria. *International Advanced Research Journal in Science, Engineering and Technology (IARJSET)*, 7(4), 1-10
13. Ampadu, S. I. K. (2007). A laboratory investigation into the effect of water content on the CBR of a subgrade soil. In *Experimental unsaturated soil mechanics* (pp. 137-144). Springer Berlin Heidelberg.
14. Ekeocha, N. E., & Akpokodje, E. G. (2012). Assessment of subgrade soils of parts of the lower Benue Trough Using California bearing ratio (CBR). *The Pacific Journal of Science and Technology*, 8, 572-579.
15. Bell, F. G. (2007). *Engineering geology*. Elsevier.
16. Bell, F. G. (2004). *Engineering geology and construction*. CRC Press.
17. Attewell, P. B., & Farmer, I. W. (2012). *Principles of engineering geology*. Springer Science & Business Media.
18. Brink, A. B. A., Parridge, J. C., & Williams, A. A. B. (1982). *Soil Survey for Engineering*, Claredon.

19. Carter, M., & Bentley, S. P. (1991). Correlations of soil properties. Pentech press publishers.
20. Clayton, C. R., Matthews, M. C., & Simons, N. E. (1982). Site investigation (No. Monograph). London: Granada.
21. De Beer, M. (1991). Use of the Dynamic Cone Penetrometer (DCP) in the design of road structures. In *Geotechnics in the African Environment* (pp. 167-176). Routledge.
22. Paige-Green, P., & Van Zyl, G. D. (2019). A review of the dcp-dn pavement design method for low volume sealed roads: development and applications. *Journal of Transportation Technologies*, 9(4), 397-422.
23. Amer, R., Saad, A., Elhafeez, T. A., Kady, H. E., & Madi, M. (2014). Geophysical and Geotechnical Investigation of Pavement Structures and Bridge Foundations. *Austin Journal of Earth Science*, 1(1), 1-6
24. Osuolale, O. M., Oseni, A. A., & Sanni, I. A. (2012). Investigation of highway pavement failure along Ibadan-Iseyin Road, Oyo State, Nigeria. *International Journal of Engineering Research & Technology (IJERT)*, 1(8), 1-6
25. Ikechukwu, A. F., Emeka, O., & Hassan, M. M. (2019). Resilient modulus prediction of subgrade soil using dynamic cone penetrometer. In *Contemporary Issues in Soil Mechanics: Proceedings of the 2nd GeoMEast International Congress and Exhibition on Sustainable Civil Infrastructures, Egypt 2018–The Official International Congress of the Soil-Structure Interaction Group in Egypt (SSIGE)* (pp. 67-87). Springer International Publishing.
26. Ikechukwu, A. F., Hassan, M. M., & Moubarak, A. (2019). Evaluation of Subgrade Resilient Modulus from Unsaturated CBR Test. In *Novel Issues on Unsaturated Soil Mechanics and Rock Engineering: Proceedings of the 2nd GeoMEast International Congress and Exhibition on Sustainable Civil Infrastructures, Egypt 2018–The Official International Congress of the Soil-Structure Interaction Group in Egypt (SSIGE)* (pp. 60-81). Springer International Publishing.
27. Chen, D. H., Lin, D. F., Pen-Hwang Liao, P. H., & Bilyeu, J. (2005). A correlation between Dynamic Cone Penetrometer values and pavement layer moduli. *Geotechnical Testing Journal*, 38 (1), 1-25.
28. Gudishala, R. (2004). Development of resilient modulus prediction models for base and subgrade pavement layers from in situ devices test results. Louisiana State University and Agricultural & Mechanical College.
29. Hassan, A. B. (1996). The effects of material parameters on Dynamic Cone Penetrometer results for fine-grained soils and granular materials. Oklahoma State University.
30. Herath, A., Mohammad, L. N., Gaspard, K., Gudishala, R., & Abu-Farsakh, M. Y. (2005). The use of dynamic cone penetrometer to predict resilient modulus of subgrade soils. In *Advances in pavement engineering* (pp. 1-16).
31. Federal Meteorological Survey (1982). Atlas of the Federal Republic of Nigeria, 2nd Edition, Federal Surveys, 160pp.
32. Illoeje, N. P. (1981). A new geography of Nigeria (New Revised Edition) published by Longman Nig. Ltd., Lagos, 201.
33. Smyth, A. J., & Montgomery, R. F. (1962). Soils and Land Use in Central Western Nigeria. *Soils and Land Use in Central Western Nigeria*, 265p
34. Wright, P. H. (1986). Highway Engineering, Sixth Edition, John Wiley and Sons, New York
35. Yoder, E. J., & Witczak, M. W. (1975). Principles of Pavement Design. 2nd Edition, John Wiley and Sons, Inc New York
36. Madedor, A. C. (1983). Pavement design guidelines and practice for different geological area in Nigeria: tropical soil of Nigeria in engineering practice, Balkema, Rotterdam, 291-297.
37. Telford, W. M., Geldart, L. P., & Sheriff, R. E. (1991). Applied Geophysics, Cambridge University Press, 792p
38. Williams, L. (1997). Fundamental of Geophysics. Cambridge University Press, 206-217
39. Kearey, P., Brooks, M., & Hill, I. (2002). An Introduction to Geophysical Exploration. Blackwell Science Limited, 262p
40. Nigeria Geological Survey (1984). Geological Map of Southwestern Nigeria, Geological Survey Department, Ministry of Mines, Power and Steel, Nigeria.
41. Nigerian Geological Survey Agency (2006). Geological and Mineral Map of Ondo State State, Nigeria
42. Zohdy, A. A. (1965). The auxiliary point method of electrical sounding interpretation, and its relationship to the Dar Zarrouk parameters. *Geophysics*, 30(4), 644-660.
43. Zhdanov, M. S., & Keller, G. V. (1994). The geoelectrical method in geophysics exploration. Elsevier, Amsterdam
44. Done, S., & Samuel, P. (2006). Department for International Development (DFID). Measuring road pavement strength and designing low volume sealed roads using the dynamic cone penetrometer. Unpublished Project Report, UPR/IE/76/06. Project Record, (R7783).
45. Hopkins, T. (1994). Minimum bearing strength of soil subgrades required to construct flexible pavements. In 4th International Conference, Bearing Capacity of Roads and Airfields FHWA, U of Minnesota, Army Corps of Engineers, NRC Canada, FAA (Vol. 1).
46. Christopher, B. R., Schwartz, C. W., Boudreaux, R., & Berg, R. R. (2006). Geotechnical aspects of pavements (No. FHWA-NHI-05-037). United States. Federal Highway Administration.
47. Kezdi, A., & Rethati, L. (1988). Handbook of Soil Mechanics, Volume 3: Soil Mechanics of Earthworks, Foundations and Highway Engineering Elsevier, Amsterdam
48. Transport and Road Research Laboratory (1990). A user's manual for a program to analyze dynamic cone penetrometer data (Overseas Road Note 8) Crowthorne: Transport Research Laboratory

49. DIN 4094 Part 2 (1980). Dynamic and Static Penetrometer
50. Lockwood, D., De Franca, V. M. P., Ringwood, B., & DeBeer, M. (1992). Analysis and classification of DCP Survey Data. Technology and Information Management Programme, CSIR Transportek, Pretoria, South Africa.
51. Chen, J., Hossain, M., & Latorella, T. M. (1999). Use of falling weight deflectometer and dynamic cone penetrometer in pavement evaluation. Transportation Research Record, 1655(1), 145-151.
52. George, K. P., & Uddin, W. (2000). Subgrade characterization for highway pavement design (No. FHWA/MS-DOT-RD-00-131). Mississippi. Department of Transportation.
53. Das, B. M. (1983). Advanced soil mechanics. New York: McGraw- Hill Book Company 442p
54. Holtz, W. G., & Kovacs, W. D. (1981). An Introduction to Geotechnical Engineering, Prentice-Hall Publishers, 733p
55. ASTM, (1990). Methods of Test for Soil for Civil Engineering Purpose. American Society for Testing and Materials.
56. Federal Ministry of Works and Housing (1997). Nigerian general specifications for roads and Bridges. Federal Highway Department, Lagos, 2, 145-284.



© Author(s) 2023. This work is distributed under <https://creativecommons.org/licenses/by-sa/4.0/>